Optimization of Continuous Enantiospecific Purification with Kinetic Modeling

A Major Qualifying Project

Submitted to the Faculty of

Worcester Polytechnic Institute

In partial fulfilment of the requirements

For the degree in Bachelor's of Science

In

Chemical Engineering

By

Griffin Carloni

Zachary Carney

Robert Dec

Date: April 27, 2023

Project Advisor: Professor Andrew Teixeira (CHE)

ACKNOWLEDGMENTS

We would like to thank Professor Andrew Teixeira for his guidance and expertise throughout our project, and for funding our work through his laboratory. We would also like to thank David Kenney, Esai Lopez, Ian Anderson, Alex Maag, Geoffrey Tompsett, and all other members of the Teixeira and Timko laboratories for their generous support of our experimentation.

ABSTRACT

While rarely used in the industrial development of pharmaceuticals, continuous flow processing offers many benefits compared to traditional batch processes such as energy efficiency, minimized chemical waste, and lower operating costs. However, more research on continuous processing is needed for companies to consider switching from traditional batch processes.

This study investigates the enantio-purification of (R,S)-1-phenylethanol in batch and flow configurations. The individual reactions comprising dynamic kinetic resolution (DKR) were studied, including kinetic resolution (KR) catalyzed by CALB Novazyme and acid-catalyzed H-Beta zeolite racemization (RAC). Reaction parameters of KR, RAC, and DKR were varied to determine optimal reaction conditions. KR and RAC reaction data was fit to Menten inhibition and pseudo-first order rate expressions. For kinetic resolution, vinyl acetate was determined to be an improved acyl donor in comparison to ethyl acetate, as observed from their fitted first order rate constants, $k'_{VA} = 3.60E\text{-}3\,\frac{L}{g_{cat}\text{-}min}$ and $k'_{EA} = 2.15E\text{-}5\,\frac{L}{g_{cat}\text{-}min}$. The optimal temperature for the racemization of 1-phenylethanol was determined to be 45°C, resulting in a 68% selectivity and an effective enantiomeric excess of 10.5%. A series packed bed reactor system with temperature control was created to optimize DKR conversion through altering recycle ratio. An optimal recycle ratio of zero was experimentally determined. Future studies should investigate the effect of racemization catalyst on RAC selectivity, alternate PBR designs, and catalyst loadings.

TABLE OF CONTENTS

Page

LIST OF TABLES

Table Page

LIST OF FIGURES

Figure Page

CHAPTER 1 Introduction

Continuous flow manufacturing has become of recent interest within pharmaceutical processing due to advantages over traditional batch processing such as decreased material and energy usage and quicker processing times (Baumann, Moody, Smyth, & Wharry, 2020). As opposed to batch processing, where raw materials and products are added and removed from a system periodically, continuous processing involves the continuous addition and removal of raw materials and products. Compared to the large vessels consistent with batch processing, continuous processing requires smaller equipment and therefore less space, allowing for efficient processes with higher throughputs per system volume, as well as reducing safety hazards (Lee, O'Connor, & Yang, 2015). The geometry of continuous flow reactors allows for more efficient heat transfer and mixing, often leading to increased yield and selectivity (Baumann, Moody, Smyth, & Wharry, 2020). Processing times are much quicker with continuous processing, adding to its increased efficiency over batch manufacturing. Finally, continuous processing allows for the use of online product analysis: active process controls can monitor system attributes and adjust control inputs accordingly, thus increasing product consistency and quality. Due to inherent quality, efficiency, and safety advantages, the FDA has encouraged the transition to continuous manufacturing within the pharmaceutical industry (Lee, O'Connor, & Yang, 2015).

Several studies have recently been published illustrating the use of continuous flow chemistry to manufacture various active pharmaceutical ingredients, or APIs (Baumann, Moody, Smyth, & Wharry, 2020). Of these studies, many have focused on the synthesis of enantiomerically pure compounds, which are increasingly in demand as building block APIs (Zhu Y. F.-L.-K., 2007). Enantioselective processes play a large role within the pharmaceutical industry, as different enantiomers of a chiral compound can induce different biological reactions. An undesired

enantiomer can produce toxic effects, as exemplified through the Thalidomide disaster of the 1950s, where the consumption of (S)-thalidomide produced teratogenic effects in pregnant women. Recent FDA guidelines strongly support the synthesis of enantiopure compounds as opposed to racemic mixtures and as a result, a majority of newly released chiral drugs are single enantiomers. Enantiospecific bio-catalysis utilizes enzymes to promote stereoselective resolutions under mild conditions and has recently emerged as a powerful tool for enantiopure synthesis. High enantiomeric excesses have been obtained in literature utilizing biocatalytic approaches such as dynamic kinetic resolution (Otvos & Kappe, 2021).

A previous MQP group at WPI researched the continuous flow production of (R)-1-phenylethylacetate (R-ester) by dynamic kinetic resolution of (R,S)-1-phenylethanol, obtaining yields of up to 38% for the R-ester product (Roche & Young, 2022). While this work measured residence time impacts on reaction yields, several other reaction parameters were not investigated. This study hopes to investigate the impacts of additional reaction parameters including acyl donor, racemization operating temperature, and recycle ratio. It was additionally sought to produce a rate law capable of modeling DKR reaction kinetics, as well as producing reactor mass balances to model conversion as a function of recycle ratio.

CHAPTER 2 Background

2.1 Dynamic Kinetic Resolution (DKR)

Kinetic resolution (KR) is a biocatalytic process that transforms one enantiomer of a racemic mixture into a product at a faster rate than the other enantiomer, resulting in an enantiopure product. Due to the stereospecific nature of KR, the maximum obtainable conversion of a racemic feedstock is 50%. While KR is able to efficiently produce enantiopure compounds, its limited yields have led to the development of an improved method: dynamic kinetic resolution (DKR). DKR combines KR with an *in-situ* racemization of the unconverted enantiomer from the starting racemic mixture. This simultaneous racemization and resolution leads to an improved theoretical racemic feedstock conversion of 100%. Successful implementation of DKR comes with several challenges, which include the difficulty of selecting racemization conditions that do not interfere with resolution (Gihani & Williams, 1999).

2.2 Reaction of study overview: DKR of (R, S)-1-Phenylethanol

1-phenylethanol is widely used throughout the pharmaceutical industry as a chiral intermediate. Several research papers have studied the DKR of racemic 1-phenylethanol using *Candida Antarctica Lipase B* (CALB) and H-beta zeolite (Habulin & Knez, 2009). The DKR of (R)-1-phenylethanol can be obtained in two steps. First, (R)-1-phenylethanol is converted to R-ester through a transesterification reaction promoted by CALB. The remaining (S)-1-phenylethanol enantiomer is then racemized by H-Beta zeolite. These two steps can be performed simultaneously or in series, depending on the design of the reactor system. CALB is the optimal enzyme for the transesterification reaction, and it is immobilized to increase thermostability. From

literature, the DKR of 1-phenylethanol was able to yield 97% of enantiomerically pure R-ester within a reaction time of 20 hours (Bogár et al., 2007).

2.3 Candida Antarctica Lipase B

Candida Antarctica Lipase B is a chiral biocatalyst used throughout the pharmaceutical industry with various applications, including the kinetic resolution of racemic sec-alcohols. The lipase structure consists of an active site made of a catalytic triad and an oxyanion hole, along with two binding pockets for the acyl-moiety of ester and alcohol parts (Cen, et al., 2018).

The two main functions of CALB are transesterification and hydrolysis. A hydrolysis reaction promoted by CALB follows a two-step mechanism. The first step is the absorption of the enzyme to a heterogeneous interface, which is followed by enhancement of the lipolytic activity (Stauch, Fisher, & Cianci, 2015). Transesterification reactions are an important function of CALB as they catalyze the resolution of racemic alcohols and are highly selective (Chen et al., 2008). A nonpolar solvent is required to increase selectivity of CALB towards the transesterification reaction. Figure 1 below depicts the transesterification of (R,S)-1-phenylethanol and vinyl acetate with CALB. The optimal temperature for CALB catalyzed transesterification was found to be 40°C in literature (Bozan , SONGÜR, & MEHMETOĞLU, 2020).

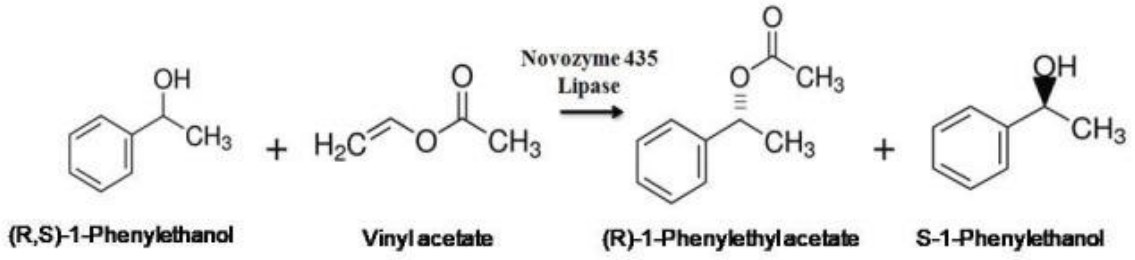

Figure 1: Dynamic kinetic resolution reaction of (R-S)-1-Phenylethanol with vinyl acetate (Bozan , SONGÜR, & MEHMETOĞLU, 2020)

2.4 Zeolite structure and function

Zeolites are crystalline, ionic, microporous structures composed of alternating SiO_4 and AlO_4 repeating units. Zeolites form naturally but can be synthesized by heating aluminosilicate gel in a very alkaline aqueous solution. Natural zeolites have a ratio of nearly five times the amount of silicon to aluminum units and may contain impurities; therefore, only synthesized zeolites are used in industry. Synthesized zeolites can have much higher Si:Al ratios. The aluminum within the structure are the components that make zeolites catalytically active by giving the structure a slight local negative charge. This negative charge is balanced by trapping alkali metal cations in the framework during the synthesis process. The H^+ ions at aluminum sites gives the zeolite acidic properties, allowing the crystalline structure to facilitate acid catalysis mechanism. Therefore, zeolite activity increases with higher amounts of aluminum in the structure. Zeolites have a structural advantage over homogenous acid catalysts due to their pores of less than 0.8nm in diameter. The fine pores highly restrict chemical availability of zeolite acid sites, which improves the selectivity of the catalyst (Jaenicke, 2007).

2.5 Zeolite racemization of 1-phenylethanol

Zeolite catalysis has been proven to be an effective method in the racemization of 1-phenylethanol compared to transition metal and biochemical methods, and zeolites are heterogenous catalysts, making product separation easier. Figure 2 below illustrates the mechanism for the acid-catalyzed racemization of 1-phenylethanol by H-beta zeolite.

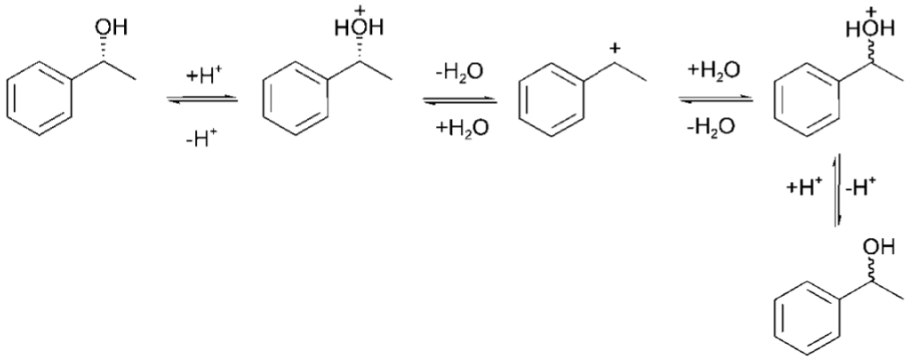

Figure 2: Acid-catalyzed racemization of 1-phenylethanol (Wuyts, De Temmerman, De Vos, & Jacobs, 2005)

The first step of the racemization begins with the protonation of the hydroxyl group on the sec-carbon, resulting in a dehydration reaction. The remaining carbocation is then re-attacked by a water molecule, with no stereospecificity. Finally, the water group becomes deprotonated, resulting in a racemic 1-phenylethanol mixture.

2.6 Packed bed reactor design and considerations

2.6.1 Packed bed reactor system components

Continuous flow heterogenous catalytic reactions are performed within packed bed reactors, or PBRs, which are tubular shells that hold an immobilized catalyst bed (Catalano, Wozniak, & Kaplan, 2022). Small scale PBRs are typically constructed of stainless-steel tubing. Several auxiliary components are required in addition to the PBR itself to allow for proper reaction control. Pumps are used to provide reactant feed to microreactors (Jensen, 2017). Static mixers are often employed at mixing junctions to promote mixing between reactant streams. Reaction temperature control is often desired and can be achieved in several ways including PBR immersion

within a heating or cooling fluid or using a heating coil. PBR temperature can be finely controlled with a proportional-integral-derivative, or PID, controller, which can control an electrical heating coil output according to a pre-defined temperature setpoint and reactor thermocouple readings. The operating pressure of a PBR can impact reaction kinetics and can also control reaction phase. By installing a back pressure regulator, or BPR, downstream of a PBR, the operating pressure of the PBR can be controlled to a given setpoint (Jensen, 2017).

2.6.2 Impacts of Catalyst Loading

The selection of a catalyst size is governed by its resulting impacts on reactor pressure drop and rate of diffusion. Smaller catalyst sizes lead to an increased pressure drop, as illustrated through the Ergun equation shown below, where D_p represents particle diameter (McCabe, Smith, & Harriott, 2005):

$$\frac{\Delta P}{L} = \frac{150 v_o \mu (1-\varepsilon)^2}{\phi_s^2 D_p^2 \varepsilon^3} + \frac{1.75 \rho v_o^2 (1-\varepsilon)}{\phi_s D_p \varepsilon^3}$$

Equation 1: Ergun equation for pressure drop through a packed bed.

Small catalyst diameters can create excessive backpressure, which in turn may overwhelm feed pumps. On the other hand, smaller catalyst sizes lead to increased external and internal diffusion rates. In diffusion limited systems, decreasing particle size will lead to an increased overall reaction rate until diffusion is no longer rate limiting (Fogler, 2020). Ideally, catalyst size should be chosen so as to prevent diffusion limitations while limiting system pressure drop.

2.6.3 Kinetic Modeling

To properly design a packed bed reactor to meet conversion requirements, an understanding of reaction kinetics is required. To completely model a DKR reactor system, rate laws for both transesterification and racemization must be understood.

Michaelis-Menten kinetics following a Ping-Pong Bi-Bi mechanism has been proposed as an acceptable model for alcohol transesterification promoted by CALB (Annapurna Devi, Radhika, & Bhargavi, 2017). The rate law consistent with this mechanism, applied to the reaction of interest, is shown below in Equation 2.

$$\frac{V}{V_{max}} = \frac{C_{RPE}C_{acyl}}{Km_{RPE}C_{acyl}\left(1 + \frac{C_{acyl}}{K_i}\right) + Km_{acyl}C_{RPE} + C_{RPE}C_{acyl}}$$

Equation 2: Ping-Pong Bi-Bi transesterification rate law

A first order rate fit can also be applied to the reaction of interest by holding the acyl donor in high molar excess, allowing for the acyl donor reaction order to approach zero in an integral fit (Fogler, 2020). For a batch reaction, first order kinetics can be modeled with Equation 3, where k' represents the pseudo rate constant and W represents catalyst weight.

$$C_{RPE} = C_{RPE_0} e^{-\frac{k'Wt}{V}}$$

Equation 3: First order batch kinetics

First order kinetics can additionally be fit to a continuous flow PBR using the model defined below in Equation 4, where τ represents residence time (Appendix A7).

$$X = 1 - \frac{1}{e^{\frac{k'\tau W}{V}}}$$

Equation 4: First order PBR flow kinetics

A past research paper investigating the effect of zeolite structure on racemization proposed first order equilibrium kinetics for concentration profiles of R and S-1-phenylethanol enantiomers. Their rate law included rate constants for evaporation rate, α, and side product formulation, k_2. The proposed rate laws are shown below in Equation 5 and Equation 6 (Costa, Lamos, Reibeiro, & Cabral, 2008).

$$\frac{\mathrm{d}\mathrm{rPE}}{\mathrm{d}t} = -k_1(\mathrm{rPE} - \mathrm{sPE}) - k_2\mathrm{rPE} + \frac{\alpha}{V}\mathrm{rPE}$$

Equation 5: (R)-1-phenylethanol racemization kinetics.

$$\frac{\mathrm{d}\mathrm{sPE}}{\mathrm{d}t} = k_1(\mathrm{rPE} - \mathrm{sPE}) - k_2\mathrm{sPE} + \frac{\alpha}{V}\mathrm{sPE}$$

Equation 6: (S)-1-phenylethanol racemization kinetics.

2.7 Reaction Sequence and Recycle Ratio

As DKR involves two separate reactions with separate catalysts, there are multiple ways to sequence the resolution and racemization steps. One study used a single PBR with alternating CALB and racemization catalyst sections separated by inert material (de Miranda, de M. Silva, & Dias, 2017). Another study used a single PBR with randomly distributed CALB and zeolite packing (Roche & Young, 2022). Alternating or randomized packing of CALB and zeolite is advantageous, as it allows for simultaneous resolution and racemization to occur throughout the PBR. A disadvantage to this scheme arises due to the different optimal operating temperatures of CALB and zeolite. Randomized packing of catalyst does not permit the presence of two separate operating temperatures, and obtaining distinct thermal gradients between alternating PBR catalyst sections is difficult.

Separate operating temperatures for CALB and H-beta zeolite can be obtained by using two PBRs in series. As the inlet feed for a DKR process is racemic, KR is performed within the first PBR, followed by a racemization PBR containing zeolite. After passing through the first PBR, assuming full conversion, 50% of the racemic 1-phenylethanol is converted to R-ester, with 50% remaining as (S)-1-phenylethanol. After passing through the second PBR, the remaining 50% (S)-

1-phenylethanol is racemized, leading to product stream containing 25% of (R)-1-phenylethanol, 25% of S-1-pheylethanol, and 50% of R-ester. Therefore, for a single pass, the maximum obtainable yield of R-ester is 50% with a maximum effective enantiomeric excess of 50%. In order to increase yield and enantiomeric excess, a recycle stream can be added from the outlet of the second PBR to the inlet of the first as illustrated in Figure 3 below.

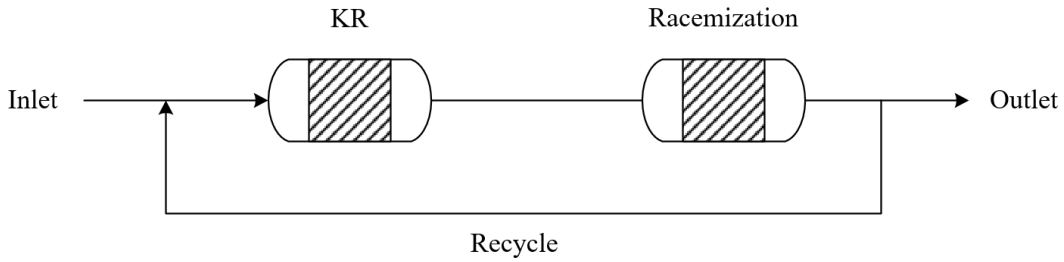

Figure 3: DKR reaction scheme with recycle stream.

Recycle ratio, defined in Equation 7, can be varied from zero to infinity. Recycle ratios of zero indicate a single pass, while a recycle ratio approaching infinity indicates a closed loop system with no outlet product stream. Increasing the recycle ratio returns (R)-1-phenylethanol produced from the racemization of (S)-1-phenylethanol to the KR PBR, theoretically resulting in increased reaction conversion.

$$Recycle\ Ratio = R = \frac{Recycle\ stream\ flowrate}{Outlet\ stream\ flowrate}$$

Equation 7: Recycle ratio.

2.8 Analytical methods

Offline Gas Chromatography-Flame Ionization Detection (GC-FID) and online Fourier Transform Infrared Spectroscopy (FTIR) were used for analytical measurements to determine reaction yields, %EE, selectivity, and steady state reaction conditions.

2.8.1 Gas Chromatography-Flame Ionization Detection

A previous MQP study optimized the following Agilent 7820 GC-FID parameters for high resolution peak separation of (R,S)-1-phenylethanol enantiomers (Roche & Young, 2022). Several parameters were studied: carrier gas, split ratio, oven temperature settings, inlet, and injection volume. A 0.25 mm inner diameter and 25 m long Agilent CP-Chirasil-Dex CB GC column was used. The optimum parameters were determined to be a split/splitless ratio of 1:100, H_2 carrier gas, 100 deg °C oven temp for 20 minutes, 5 mg/mL concentration, and an injection volume of 0.2 µL.

GC FID standard curve calibrations can be made accurately using an internal standard. The internal standard will account for any differences in injection volume, evaporation of the sample, or small differences in operation conditions of the reactor and GC-FID. Internal standards are important when working with small concentrations to minimize error.

Equation 8: Internal standard ratio below shows the relationship between analyte and internal standard signal responses to concentrations, where the subscript x represents the unknown analyte and the subscript s represents the internal standard (Mullaugh, 2020). A calibration curve can be created to find the ratio between the responses, F, which can then be used to calculate species concentration given a known internal standard volume.

$$\frac{P.A_{R-PE}}{[R-PE]} = F\frac{P.A_{Anisole}}{[Anisole]}$$

Equation 8: Internal standard ratio

2.8.2 Inline FTIR

In continuous flow reaction systems, reactants can undergo several changes from when they enter and exit the system. Therefore, a way of monitoring the reaction kinetics for changes in reaction parameters could be inline or online FTIR monitoring. Inline monitoring refers to the insertion of an infrared (IR) probe into the flow. Online monitoring refers to the small diversion of the product stream to an IR analyzer. If the reactants and products do not have IR spectra peak overlaps, then the conversion of the reaction can be seen in real time with the use of reactant and product standard calibration curves. The specific reaction of interest that has the potential for online IR measurements is the KR of 1-phenylethanol into R-ester by monitoring the acyl donor concentration. Standard calibration curves can be made for inline or online FTIR using dilutions in the concentration range that will be studied. A prominent peak that does not overlap with other reactant or product spectra must be identified to create a calibration curve of the reaction system. The observed peak absorbance will have a proportional relationship to concentration.

CHAPTER 3 Experimental Procedures

3.1 Analytical Methods

3.1.1 ReactIR

Mettler Toledo ReactIR © software was used throughout experimentation to monitor KR reaction progress in real time. Prior to constructing calibration curves, analyte solutions were first run to produce a series of spectrums. The spectra of each solution were then overlaid to identify prominent peaks of interest for each compound. Calibration curves were then created for each analyte by varying analyte concentration in toluene and measuring the change in absorbance at corresponding peaks of interest. A calibration model for each applicable compound was created using the ReactIR © software.

3.1.2 Gas Chromatography

GC was used in addition to flow IR for reaction analytics. While IR is unable to discern between enantiomers, GC utilizes chromatographic separation to measure separate concentrations. An Agilent 7820A GC with an Agilent CP-Chirasil-DEX CB 0.25mm x 25 m chiral column was utilized for steady state sample measurements. Prior to constructing calibration curves, GC parameters were varied to optimize racemic 1-phenylethanol separation. A series of analyte solutions were then run through the GC to determine retention times for each compound. While constructing calibration curves, an internal standard, anisole, was added in known concentration to each sample. Anisole was chosen as an internal standard due to shared chemical properties with the analytes of interest and chemical stability throughout the reaction system.

3.2 Flow Reactor System Set-Ups

For both KR and racemization flow studies, a continuous flow system was constructed with a single PBR filled with either CALB or H-Beta zeolite. A Vici-Valco M6 series positive displacement pump was connected to a feed vial containing reagent solution. Inlet and outlet tubing from the feed pump was $1/16^{th}$ inch PFA tubing. Outlet tubing from the pump was then connected to KR or racemization PBR using a Swagelok fitting. PBRs were constructed of stainless-steel tubing, with stainless steel frits threaded on either end to prevent loss of catalyst. PBR temperatures were controlled with an Omega © temperature controller. A K-type thermocouple taped along the length of the PBR and covered with heating tape and insulation provided temperature input to the controller. Outlet tubing was then connected to an IR flow cell prior to exiting into a collection vial.

For DKR studies, two PBRs were placed in series. The first PBR was filled with CALB to promote KR. Outlet tubing from this reactor was connected to a second PBR filled with H-beta zeolite for racemization. The outlet from the racemization PBR was then connected to the IR flow cell and collection vial. For DKR recycle ratio studies, a second Vici-Valco pump was used to recycle fluid from the tee of the second PBR to a tee between the feed pump and first PBR. A piping and instrumentation diagram (P&ID) for the DKR system with a recycle pump is included below within *Figure 4.*

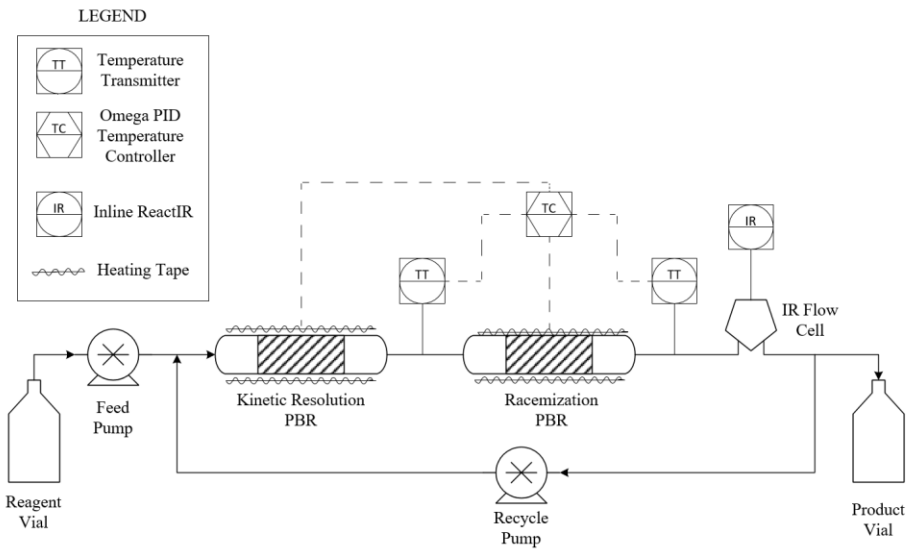

Figure 4: P&ID for dynamic kinetic resolution reaction system.

3.3 Effect of Acyl Donor on Batch KR

The effect of acyl donor on kinetic resolution kinetics was first investigated within a batch configuration. Kinetic resolution was first performed using ethyl acetate as the acyl donor. A 10 mL solution was prepared with 30 mg/mL ethyl acetate, 30 mg/mL (R,S)-1-phenylethanol, and 15 mg/mL anisole. The solution was added to a 25 mL beaker containing approximately 315 mg of CALB. Heating tape was taped around the beaker, and a thermocouple was placed into the reaction solution. Reaction temperature was maintained at 40°C using an Omega © PID temperature controller. A stir bar was used to ensure proper mixing of the reaction solution. This reaction was repeated with vinyl acetate. Catalyst loading was increased for the vinyl acetate reaction to approximately 80 mg CALB per mL solution. Reaction samples for both acyl donors were taken intermittently throughout the experiment for use within kinetic rate law fitting. Excel Solver was used to fit kinetic rate parameters for both first order and Michaelis-Menten models.

3.4 Effect of Acyl Donor on Continuous Flow KR

To determine the effect of acyl donor on kinetic resolution in flow, a reaction system resembling Figure 4 was constructed without the recycle stream and racemization PBR. Several trials were run, varying acyl donor between vinyl and ethyl acetate. Inlet concentrations of both the acyl donor and racemic 1-phenylethanol were held at 30 mg/mL throughout all trials, resulting in a nearly 3:1 molar ratio of acyl donor to (R)-1-phenylethanol. The residence time of study was varied between 0.5 and 15 minutes by varying inlet flowrate according to Appendix A1. The KR PBR was constructed to a length and diameter of 10 cm and 4 mm, respectively. CALB was wet packed into the column by adding, dropwise, a slurry of toluene and CALB resin beads. Approximately 602 mg of CALB enzyme was added to the column. A reaction temperature of 40°C was chosen to mimic optimal conditions (Sigma Aldrich, 2022). ReactIR © was used to monitor reaction progress and indicate when steady state conditions were reached. Steady state product samples were taken for GC analysis. Table 1 summarizes the varied reaction conditions for each trial. For each trial, conversion, yield, and effective enantiomeric excess were recorded. Conversion data was used to fit reaction rate parameters for flow kinetics.

Table 1: Reaction parameters for acyl donor kinetic resolution experiment.

Trial	Acyl Donor	Residence Time [min]
1	Ethyl Acetate	5
2	Ethyl Acetate	10
3	Ethyl Acetate	15
4	Vinyl Acetate	0.5
5	Vinyl Acetate	2.5
6	Vinyl Acetate	5
7	Vinyl Acetate	10
8	Vinyl Acetate	15

3.5 Validation of Racemization in Batch

To ensure the effectiveness of the racemization catalyst prior to continuous flow experimentation, racemization was first conducted in a batch reactor system. Product solution from the batch kinetic resolution reaction with vinyl acetate, with an effective enantiomeric excess of 100%, was used as a starting feed for the racemization. H-beta zeolite was first sieved to a catalyst size between 100-150 µm. Approximately 37.8 mg of zeolite was added with 7.6 mL of product solution to a 25 mL beaker. Heating tape was used to control the reaction temperature to 45°C. A stir bar was utilized to ensure proper mixing. Reaction solution samples were taken periodically for over two hours for rate law fitting purposes. Concentration versus time data was fitted to first order reversible kinetics using Excel Solver.

3.6 Effect of Temperature on Continuous Flow Racemization

The effect of temperature on continuous flow racemization was studied through the modified experimental design as seen in Figure 4. The modified system design included all components except the kinetic resolution PBR and thermocouple, recycle loop, and IR flow cell. The racemization PBR had dimensions of 14.5 cm length by 0.94 cm inner diameter and was dry packed with about 2.1 g of H-Beta Zeolite sieved to 100-150 μm. Heating tape was wrapped around the racemization PBR to maintain a constant temperature**.** Reactant feed for racemization trials was used from previous kinetic resolution batch reactions, as a high enantiomeric excess of (S)-1-phenlyethanol was desired. Feed flowrate was set for a constant residence time of 60 minutes across all trials. Racemization temperatures varied between 45°C-75°C, according to Table 2.

Table 2: Racemization temperature trials

Trial	Temperature [°C]
1	45
2	60
3	75

3.7 Effect of Recycle Ratio on DKR

A DKR reaction system was constructed according to Figure 4. The kinetic resolution PBR was wet packed with CALB while the racemization PBR was packed with H-beta zeolite. The racemization PBR was controlled to its optimal temperature experimentally found from Section 3.6, while the KR PBR was held at 40°C. The KR PBR size was held at 10 cm length and 4 mm

inner diameter. The racemization PBR column dimensions were 14.5 cm length and 9.4 mm diameter, allowing for a higher residence time than the KR PBR. For each trial, the optimal acyl donor experimentally found from Section 3.3 was fed to the system with racemic 1-phenylethanol in toluene. Inlet concentrations for the acyl donor and racemic 1-phenlyethanol were both held at 30 mg/mL. The inlet flowrate of reagent into the system was held constant throughout all trials at 0.5 mL/min, and steady state was allowed to be reached for each trial. The main variable of study between trials was recycle ratio, which was adjusted by varying recycle pump flowrate according to A6. Recycle ratio flowrate. Table 3 summarizes the reaction parameters for each trial. Reaction conversion, yield, and enantiomeric excess was recorded for each trial.

Table 3: Reaction parameters for recycle ratio DKR experiment.

Trial	**Recycle Ratio**
1	0
2	10
3	50

CHAPTER 4 Discussion of Results

4.1 Analytical methods results.

4.1.1 Online Infrared Spectroscopy

Figure 5 below shows the obtained spectrum for pure toluene. Distinct peaks can be observed around 1500 cm^{-1} and 600 cm^{-1} wavelengths.

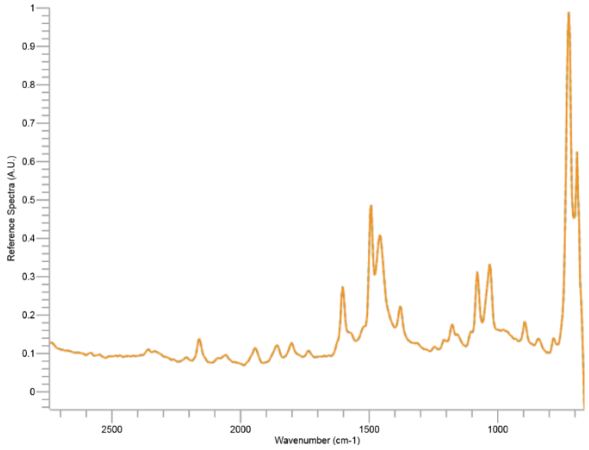

Figure 5: Pure toluene IR spectrum

A 30 mg/mL solution of ethyl acetate was then run, with the toluene spectrum subtracted as a background, resulting in the spectrum shown in Figure 6. Distinct peaks were observed near 1700 cm^{-1} and 1200 cm^{-1}. A similar spectrum was obtained for a 30 mg/mL vinyl acetate solution (Appendix B).

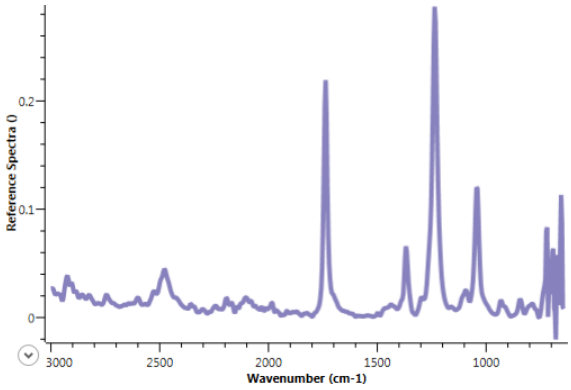

Figure 6: 30 mg/mL ethyl acetate in toluene

The racemic 1-phenylethanol solution was additionally run, but no unique peaks were observed. A sample taken from the ethyl acetate batch kinetic resolution trial was additionally sampled, with no distinct peaks existing for the R-ester product (Appendix B). Calibration curves were then constructed for both vinyl and ethyl acetate within Mettler Toledo ReactIR © software.

4.1.2 Gas Chromatography Flame Ionization Detection

GC oven parameters were varied until complete separation of all peaks was observed. The final optimized parameters chosen for GC operation are summarized within Appendix E.

Retention times for each compound are summarized below within

Table 4 . Retention times were taken from initial injection to the highest point of each eluted peak. Appendix C shows GC chromatograms of each sample.

Table 4: GC retention times

Compound	Retention Time [min]

Vinyl Acetate	1.2
Ethyl Acetate	1.2
Toluene	1.5
Anisole	2.3
R-ester	7.3
(R)-1-Phenylethanol	9.6
(S)-1-Phenylethanol	10.4

Calibration curves were constructed using an internal standard of anisole. Curves were plotted on Excel and are shown in Appendix D.

4.2 Effect of Acyl Donor on Batch KR

The first batch reaction ran used ethyl acetate as the kinetic resolution acyl donor. A (R)-1-phenylethanol conversion of approximately 40% was obtained after 120 minutes of reaction time. For the vinyl acetate batch reaction, a conversion of nearly 85% was reached after 120 minutes. In order to account for catalyst loading differences, kinetic parameters between the acyl donors were compared. Concentration versus time data for kinetic resolution reactions with both ethyl and vinyl acetate acyl donors were fit to 1^{st} order and Michaelis-Menten kinetics, resulting in the reaction rate parameters displayed in Table 5.

Table 5: Batch kinetic resolution kinetic parameters

Acyl Donor	1st Order	Michaelis Menten			
	$k' \left[\frac{L}{g\text{-}min}\right]$	$V_{max}[\frac{mol}{g\text{-}min}]$	$K_{mRPE}\ [M]$	$K_{mAcyl}\ [M]$	K_I [M]
Ethyl Acetate	1.50E-4	24.7	1.80	1.12	0.001
Vinyl Acetate	6.00E-4	43.4	1.10	0.001	0.001

Both the first order pseudo rate constant and Menten V_{max} parameters for vinyl acetate were considerably higher than those determined for ethyl acetate, showing that vinyl acetate produces faster transesterification kinetics. **Error! Reference source not found.** shows concentration versus time fits for first order and Menten kinetic rate expressions. While both models produced similar fits, the first order approximation was superior at modeling ethyl acetate concentrations at longer reaction times.

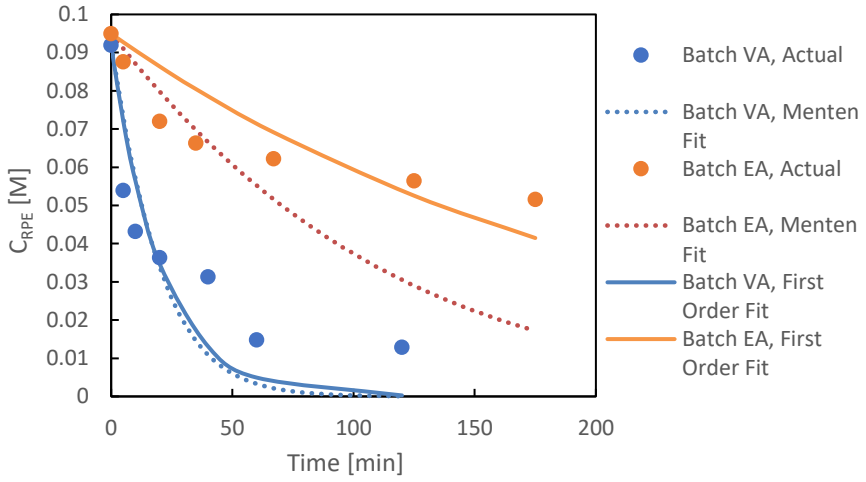

Figure 7: Batch kinetic resolution fits

4.3 Effect of Acyl Donor on Continuous Flow Kinetic Resolution

Figure 8 and Figure 9 show flow KR reaction metrics as a function of residence time for both ethyl acetate and vinyl acetate acyl donors. As the residence time was increased, R-PE conversion increased for both acyl donors. The three residence times studied for vinyl acetate recorded an average R-PE conversion between 84% and 93%, while ethyl acetate was between 14.7% and 27.1%. The average EE% for vinyl acetate was between 75% and 88%, while ethyl EE% was between 7.9% and 18.6%. The purpose of the experiment was to determine which acyl donor would yield more of the desired product. Overall, vinyl acetate as an acyl donor resulted in a higher (R)-1-phenylethanol conversion and %EE compared to ethyl acetate. It was therefore determined to conduct the experiments that followed with vinyl acetate.

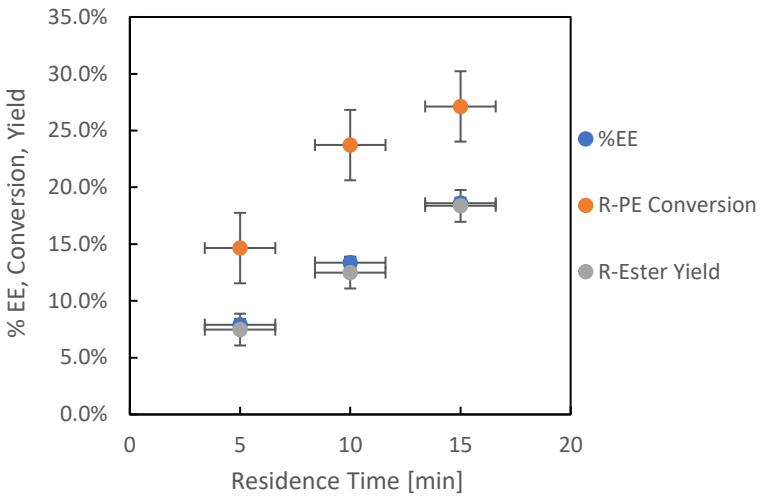

Figure 8. Kinetic resolution of R,S PE in flow using ethyl acetate as the acyl donor at 3 different residence times.

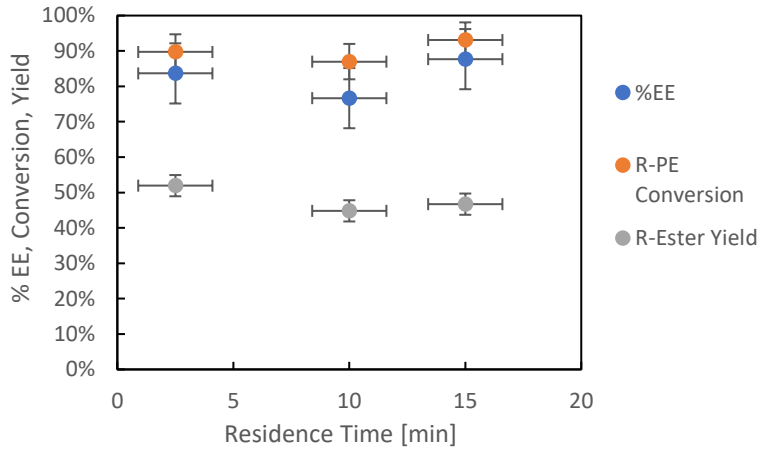

Figure 9: Kinetic resolution of R,S PE in flow using Vinyl Acetate as the acyl donor at 3 different residence times.

Kinetic data from batch KR experiments was used to predict conversion within a flow reactor using methods outlined in Appendix A9. The predicted conversion profiles are shown in **Error! Reference source not found.**. Both first order and Menten predicted conversion profiles

overestimate (R)-1-phenlyethanol conversion with ethyl acetate by up to 200% for higher residence times.

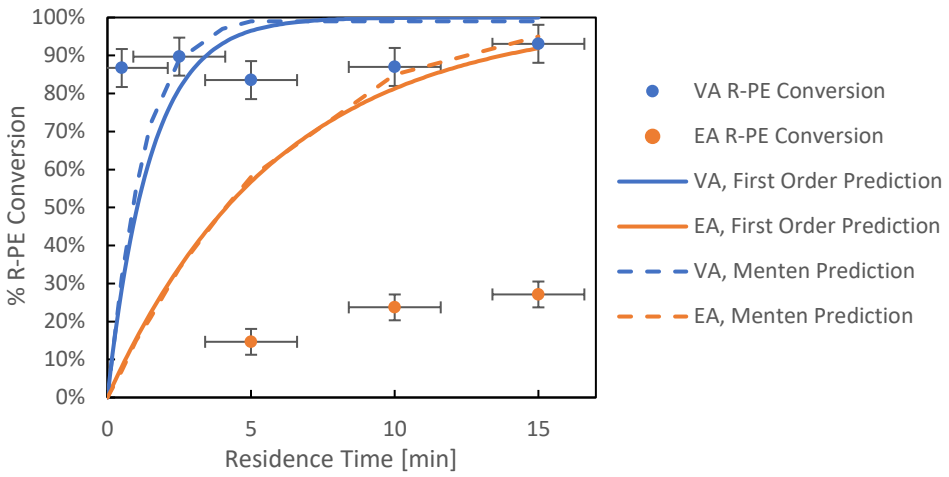

Figure 10: Flow kinetic resolution predicted conversions from batch kinetic parameters.

Rate expressions were then fitted to flow data to produce a new set of flow derived kinetic parameters summarized within Table 6. These parameters resulted in the conversion versus residence time fits shown in Figure 11 below.

Table 6: Kinetic resolution continuous flow, fitted kinetic parameters.

Acyl Donor	1st Order	Michaelis Menten			
	$k'\left[\frac{L}{g\text{-}min}\right]$	$V_{max}[\frac{mol}{g\text{-}min}]$	$K_{mRPE}\,[M]$	$K_{mAcyl}\,[M]$	K_I [M]
Ethyl Acetate	2.15E-5	56.8	1.80	1.10	0.00
Vinyl Acetate	3.60E-3	2750.0	1.10	0.00	0.00

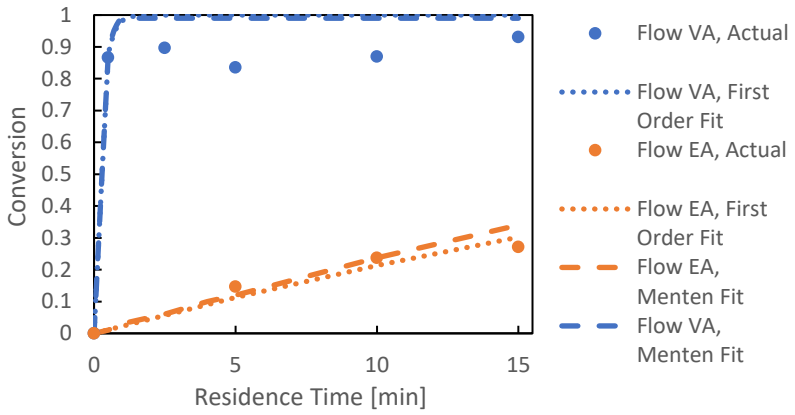

Figure 11: Conversion versus residence time, kinetic resolution fits

Observed from Figure 11, both first order and Menten approximations fits resulted in good agreement with kinetic resolution flow data.

4.4 Racemization in Batch

The racemization reaction was performed in batch at 45°C for 80 minutes. Five samples were taken at 0, 10, 20, 40, and 80 minutes. The time samples were analyzed using GC-FID to determine concentration of each enantiomer as the reaction progressed as seen in **Error! Reference source not found.** (S)-1-phenylethanol decreased from an initial concentration to 0.09M to 0.06M, and (R)-1-phenylethanol increased from an initial concentration of 0M to 0.015M. Therefore, part of (S)-1-phenylethanol went to a side reaction during RAC.

A kinetic analysis was performed by fitting batch RAC concentration versus time data against Equation 5 and Equation 6. The alpha term modeling solvent evaporation was omitted from the equation for simplification. Table 7 summarizes the fitted kinetic RAC parameters, while Figure 12 plots obtained fits against experimental data.

Table 7: First order reversible kinetic parameters obtained for batch (S)-1-phenylethanol racemization.

1st Order

k_1 $[\frac{L}{g_{cat}\text{-}min}]$	k_2 $[\frac{L}{g_{cat}\text{-}min}]$
0.005865	0.0068663

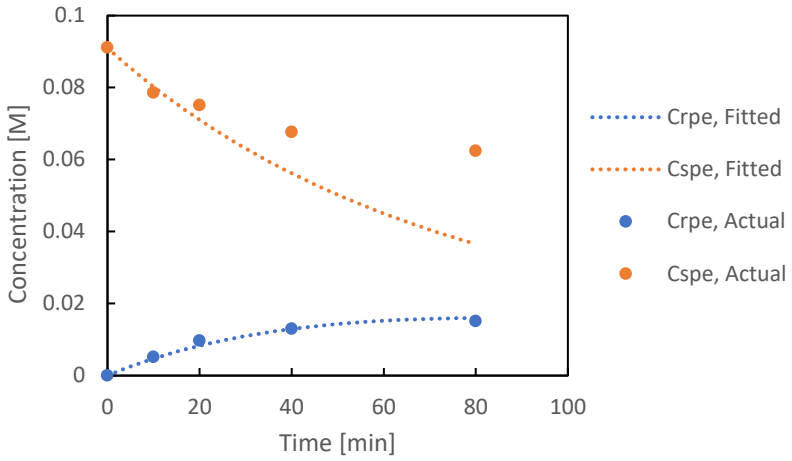

Figure 12: Racemization in batch of concentration of (R)- and (S)-1-phenylethanol versus time for 5 samples.

4.5 Racemization in Continuous Flow

The RAC reaction of (S)-1-phenylethanol at temperatures of 45-, 60-, and 75°C resulted in a decreasing trend of %EE and selectivity of the desired reaction (Figure 13). For 75°C, %EE was approximately zero and selectivity was 30%, meaning most of the reactants followed an undesired side reaction. At 60°C, %EE was approximately 7% and selectivity was 60%. At 45°C, %EE was approximately 10% and selectivity was 68%. Therefore, the study of temperatures effect on racemization revealed decreased selectivity of the desired reaction as temperature increased, but higher conversions of (S)-1-phenylethanol at higher temperatures. Since the reaction will be run in a DKR system, it is desired to have high selectivity to prevent buildup of undesired products, showing that the optimal racemization temperature was 45°C. Outlet concentrations from each trial were used to fit racemization kinetic parameters using concentration equations described in Appendix A10. The impact of temperature on kinetic parameters are summarized in Table 8. Fitted parameters also indicated that as temperature increased, the selectivity of the racemization reaction

decreased, shown by the decreasing ratio between the RAC rate constant, k_1, and the side product formation rate constant, k_2.

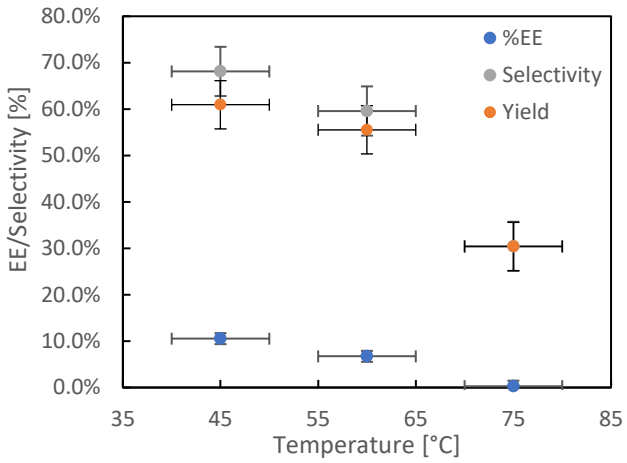

Figure 13. Effect of temperature on racemization of S-PE at 3 different temperatures, 60-minute residence time, with %EE and selectivity of the reaction plotted.

Table 8: First order reversible racemization with side product formation continuous flow kinetic fit

Temperature [°C]	k_1 $[\frac{L}{g_{cat}\text{-}min}]$	k_2 $[\frac{L}{g_{cat}\text{-}min}]$
45	4.3E-6	1.7E-6
60	3.3E-6	3.3E-6
75	1.4E-5	4.8E-6

4.6 Effect of Recycle Ratio on Dynamic Kinetic Resolution

The highest conversion for DKR was observed under no recycle operating conditions, and decreased as recycle ratio was increased. The study on the effect of recycle ratio on DKR was conducted using recycle ratios of 0, 10 and 50 (Figure 14). A theoretical prediction on the effect of recycle ratio on conversion was created with mathematical model using kinetic parameters obtained for flow KR and RAC (Appendix A11). The predicted outcome of increasing recycle ratio was an increase in R-ester yield as an increase in recycle ratio would allow for more conversion of unreacted species. 3.2 It was observed, however, that as recycle ratio increased there was a decrease in R-ester yield, enantiomeric excess, and (R,S)-1-phenylethanol conversion. The unexpected outcome may have been due to a side reaction in the racemization PBR, as there would be more racemization reactions occurring at higher recycles, or inaccuracies in the rate expressions used within the prediction model.

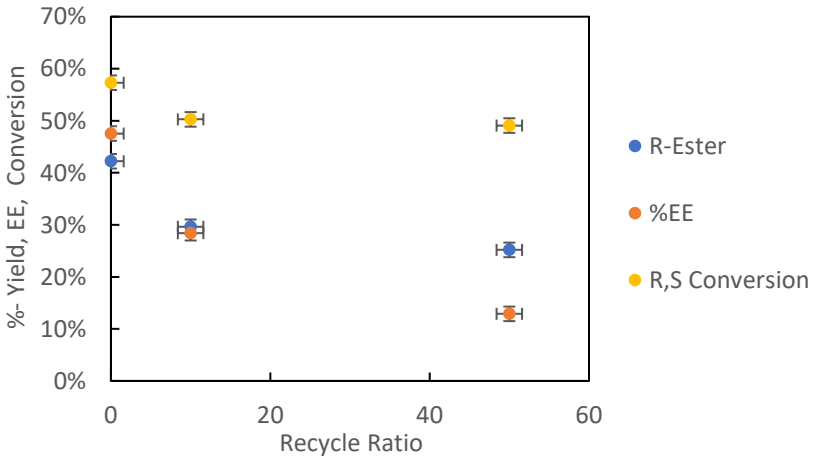

Figure 14. Effect of recycle ratio on DKR conversion showing the highest conversions when the system was operated under no recycle.

CHAPTER 5 Conclusion and Recommendations

5.1 Conclusions

This project aimed to optimize the flow reactor system of dynamic kinetic resolution to perform enantio-purification of (R,S)-1-phenylethanol using *candida antarctica lipase B* and H-beta zeolite. The optimization was performed through kinetic resolution and racemization reactions in batch and flow by varying acyl donor, temperature, residence time, and recycle ratio. Experiments were analyzed using an adjusted offline gas chromatography method for the chiral separation of (R)- and (S)-1-phenylethanol. Analysis also utilized inline FTIR analysis of the kinetic resolution reaction to monitor steady state conditions.

The optimization of flow dynamic kinetic resolution requires further study, but this work is significant. This study conveys the benefits of continuous flow reactors, reaching higher conversions and producing less waste than batch. This work additionally exemplified how a reaction can be switched from batch to continuous flow through the use of reaction engineering principles. With further research, the pharmaceutical industry can take advantage of flow processing and cut down on waste and operating costs.

5.2 Recommendations

Future research on DKR flow chemistry should be explored for the racemization reaction, recycle ratio, and alternate catalyst/enzyme packing methods. It is also recommended to install a pressure gauge on the reaction system as a safety measure to prevent pressure buildup and tubing ruptures caused by catalyst caking within the reactor.

The racemization of (R,S)-1-phenylethanol was studied under different reaction temperatures. The result of this experiment conveyed that increasing temperature achieved lower enantiomeric excess and decreased selectivity. Therefore, future studies can be performed on improving the selectivity of the (S)-1-phenylethanol racemization in order to achieve improved enantio-purification of (R,S)-1-phenylethanol in a DKR reaction system.

Recycle ratio was studied with the expected outcome of improving enantio-purification as recycle ratio increased. However, the increasing recycle ratio decreased conversion and product yield. Therefore, more experimentation on the effect of a recycle stream on the system should be investigated to improve enantio-purification.

In literature there are many different catalyst and enzyme loading designs for DKR. Our project utilized two PBRs, the first loaded with CALB enzyme for KR, and the second with H-Beta zeolite for RAC. This reactor sequencing was chosen so that each reaction could be run under its catalyst's optimum operating temperature. However, after studying the effect of temperature on RAC, we recommend investigating alternative configurations and loading designs for improving DKR. Specifically, since optimal catalyst operating temperatures were very close, using one PBR with alternating CALB and H-Beta zeolite packing separated by quartz wool may improve DKR yield. RAC is the slow step of DKR; therefore, packing ratio of CALB and H-Beta zeolite should also be investigated.

APPENDICES

APPENDIX A – Calculations

A1. Residence time.

Finding volumetric flowrate to achieve a given residence time.

$$\tau = \frac{\mathrm{V}}{\dot{V}} \rightarrow \dot{V} = \frac{V}{\tau}$$

$$V = \pi r^2 L \varepsilon$$

Where ε is void fraction of the packing and V is void space volume.

Given a 4 mm diameter, 10 cm long PBR:

$$r = \frac{D}{2} = \frac{4.0mm}{2} = 2.0mm$$

$$L = 10.0\ cm$$

Given a void fraction of approximately 0.38 (McCabe, Smith, & Harriott, 2005).

$$\varepsilon = 0.38$$

$$V = \pi \left[(2mm)\left(\frac{1cm}{10mm}\right)\right]^2 (10cm)(0.5) = 0.63cm^3 = 0.63mL$$

$$\tau = 15min$$

$$\dot{V} = \frac{0.63mL}{15min} = 0.042\frac{mL}{min}$$

A2. PBR pressure drop.

Pressure drop through a packed bed can be modeled by the Ergun Equation. The following calculations are performed for a H-beta zeolite packed PBR.

$$\frac{\Delta P}{L} = \frac{150 v_o \mu (1-\varepsilon)^2}{\phi_s^2 D_p^2 \varepsilon^3} + \frac{1.75 \rho v_o^2 (1-\varepsilon)}{\phi_s D_p \varepsilon^3}$$

$$L = PBR\ length = 10\ cm = 0.10\ m$$

$$v_o = Superficial\ velocity = \frac{\dot{V}}{A} = \frac{0.042 \frac{cm^3}{min}}{\pi (0.2cm)^2} = 0.334 \frac{cm}{min} \approx 5.57E\text{-}5 \frac{m}{s}$$

$$\phi_s = Particle\ sphericity \approx 0.65$$

$$D_p = 0.125\ mm = 1.25E\text{-}4\ m$$

$$\varepsilon = 0.38$$

$$\rho \approx \rho_{toluene} = 867 \frac{kg}{m^3}$$

$$\mu = 419E\text{-}6\ Pa\text{-}s$$

$$\frac{\Delta P}{L} = \frac{150 \left(5.57E\text{-}5 \frac{m}{s}\right) (419E\text{-}6\ Pa\text{-s})(1-.38)^2}{(0.65)^2 (1.25E\text{-}4m)^2 (0.38)^3} + \frac{1.75 \left(867 \frac{kg}{m^3}\right) \left(5.57E\text{-}5 \frac{m}{s}\right)^2 (1-.38)}{(0.65)(1.25E\text{-}4m)(0.38)^3}$$

$$\frac{\Delta P}{L} \approx 3715 \frac{Pa}{m} \rightarrow \Delta P = \left(3715 \frac{Pa}{m}\right)(0.10m) = 371.5\ Pa = 0.054\ psi$$

A3. Effective enantiomeric excess.

$$C_{R_{PE}} = 0.1\ M$$

$$C_{S_{PE}} = 0.1\ M$$

$$C_{R_{phenylacetate}} = 0.1\ M$$

$$\%EE = \frac{\left|C_{R_{PE}} + C_{R_{phenylacetate}} - C_{S_{PE}}\right|}{C_{R_{PE}} + C_{R_{phenylacetate}} + C_{S_{PE}}}$$

$$\%EE = \frac{|0.1M + 0.1M - 0.1M|}{0.3M} = 33.3\%$$

A4. Effective yield of R-ester.

$$C_{R-ester} = 0.1M$$

$$C_{(R)-alcohol} = 0.1M$$

$$C_{(S)-alcohol} = 0.1M$$

$$Effective\ yield = \frac{C_{R-ester}}{C_{(R)-alcohol} + C_{(S)-alcohol}}$$

$$Effective\ yield = \frac{0.1M}{(0.1 + 0.1)M} = 0.5$$

A5. Reaction conversion and Selectivity.

$$PE\ Conversion = \frac{moles\ reacted\ (R,S)\text{-}1\text{-}phenylethanol}{moles\ fed\ (R,S)\text{-}1\text{-}Phenylethanol}$$

$$\frac{0.004\ moles\ reacted\ (R,S)\text{-}1\text{-}phenylethanol}{0.009\ moles\ (R,S)\ 1\text{-}Phenylethanol} = 44.4\%\ Conversion$$

$$R - PE\ Conversion = \frac{moles\ reacted\ (R)\text{-}1\text{-}phenylethanol}{moles\ fed\ (R)\text{-}1\text{-}phenylethanol}$$

$$\frac{0.004\ moles\ \text{reacted}\ (R)\text{-}1\text{-}phenylethanol}{0.0045\ moles\ (R)\text{-}1\text{-}Phenylethanol} = 89.0\%\ Conversion$$

$$Racemization\ Selectivity = \frac{(C_{R-Pe} + C_{S-Pe})_{out}}{(C_{R-Pe} + C_{S-Pe})_{in}}$$

$$\frac{(0.1 + 0.1)\text{M}}{(0.1 + 0.1)\text{M}} = 100\%\ Selectivity$$

A6. Recycle ratio flowrate.

$$Recycle\ Ratio = R = \frac{\dot{V}_{recycle}}{\dot{V}_{outlet}}$$

At steady state:

$$\dot{m}_{in} = \dot{m}_{outlet}$$

Assuming constant density:

$$\dot{V}_{in} = \dot{V}_{outlet} = 0.042 \frac{mL}{min}$$

Given recycle ratio of 5:

$$\dot{V}_{recycle} = 0.21 \frac{mL}{min}$$

A7. Internal standard.

$$\frac{P.A_{R-PE}}{[R\text{-}PE]} = F * \frac{P.A_{Anisole}}{[Anisole]}$$

The peak areas of R-PE and Anisole are known, as well as Anisole concentration, therefore the adjusted concentration of R-PE can be determined using the internal standard. The response factor F, was determined by preparing known concentrations of R-PE and Anisole.

A8. First order flow KR expression.

Starting with the design equation for a PBR reactor, where A represents (R)-1-phenylethanol (Fogler, 2020):

$$\frac{dX}{dW} = \frac{-r'_A}{F_{A0}} = \frac{k'C_A}{C_{A0}\dot{V}_0}$$

Rewriting in terms of conversion, substituting in residence time, τ:

$$\frac{dX}{dW} = \frac{k'C_{A0}(1-X)\tau}{C_{A0}V} = \frac{k'(1-X)\tau}{V}$$

Solving differential equation with X(0)=0 and W(0)=0:

$$X = 1 - \frac{1}{e^{\frac{k'\tau W}{V}}}$$

A9. Predicting continuous flow conversion from batch kinetic parameters.

Kinetic resolution conversion within a continuous flow reactor was predicted from kinetic parameters obtained from batch experimentation. From batch KR experiments, $k'_{VA} = 6.00\text{E-}4\ [\frac{\text{L}}{g_{cat}-min}]$.

Given a catalyst loading of $W = 0.600\ g$, a volume of $V = 0.537E\text{-}3\ L$, and a residence time of $\tau = 5\ min$:

$$X = 1 - \frac{1}{e^{\frac{k'\tau W}{V}}}$$

$$X = 1 - \frac{1}{e^{\frac{(6.00E-4\left[\frac{L}{g_{cat}\text{-}min}\right])(5\text{min})(0.600\text{g})}{(0.537E\text{-}3L)}}}$$

$$X \approx 96.5\%$$

A10. Continuous flow racemization differential equation solutions.

Continuous flow racemization differential equations were defined from PBR design equations (Fogler, 2020).

$$\frac{dF_{RPE}}{dW} = r'_{RPE}$$

$$r'_{RPE} = -k_1 C_{RPE} + k_1 C_{SPE} - k_2 C_{RPE}$$

$$F_{RPE} = C_{RPE}\dot{V}$$

$$\frac{dC_{RPE}}{dW} = \frac{-k_1 C_{RPE} + k_1 C_{SPE} - k_2 C_{RPE}}{\dot{V}}$$

Similar differential equations were created for (S)-1-phenylethanol and the unknown side product species.

These differential equations were solved within MATLAB, resulting in the following equations:

$$C_{RPE} = \left(e^{\frac{-[(W)(2k_1+k_2)}{\dot{V}}}\right)\left(\frac{C_{RPE0}}{2} - \frac{C_{SPE0}}{2}\right) + \frac{e^{\frac{-(k_2 W)}{\dot{V}}}(C_{RPE0} + C_{SPE0})}{2}$$

$$C_{SPE} = \frac{e^{\frac{-(k_2 W)}{\dot{V}}}(C_{RPE0} + C_{SPE0})}{2} - \left(e^{\frac{-[W)(2k_1+k_2)}{\dot{V}}}\right)\left(\frac{C_{RPE0}}{2} - \frac{C_{SPE0}}{2}\right)$$

$$C_{side\ product} = C_{side\ product\ 0} + C_{RPE0} + C_{SPE0} - e^{\frac{-(k_2 W)}{\dot{V}}}(C_{RPE0} + C_{SPE0})$$

A11. DKR recycle ratio model.

A DKR model was created within Excel using reactor balances and first order rate expressions. Kinetic parameters for the individual KR and RAC reactions with vinyl acetate were obtained within Section 4.3 and 4.5, respectively, and are shown below:

$$k'_{KR} = 3.60E\text{-}3\ [\frac{L}{g_{cat}\text{-}min}]$$

$$k_{1_{RAC,45C}} = 4.3E\text{-}6\ [\frac{L}{g_{cat}\text{-}min}]$$

$$k_{2_{RAC,45C}} = 1.7E\text{-}6\ [\frac{L}{g_{cat}\text{-}min}]$$

The following rate expressions were used:

$$X_{KR} = 1 - \frac{1}{e^{\frac{k'\tau W}{V}}}$$

$$C_{RPE} = \left(e^{\frac{-[(W)(2k_1+k_2)}{\dot{V}}}\right)\left(\frac{C_{RPE0}}{2} - \frac{C_{SPE0}}{2}\right) + \frac{e^{\frac{-(k_2W)}{\dot{V}}}(C_{RPE0} + C_{SPE0})}{2}$$

$$C_{SPE} = \frac{e^{\frac{-(k_2W)}{\dot{V}}}(C_{RPE0} + C_{SPE0})}{2} - \left(e^{\frac{-[W)(2k_1+k_2)}{\dot{V}}}\right)\left(\frac{C_{RPE0}}{2} - \frac{C_{SPE0}}{2}\right)$$

$$C_{side\ product} = C_{side\ product\ 0} + C_{RPE0} + C_{SPE0} - e^{\frac{-(k_2W)}{\dot{V}}}(C_{RPE0} + C_{SPE0})$$

The iterative Excel sheet below was created:

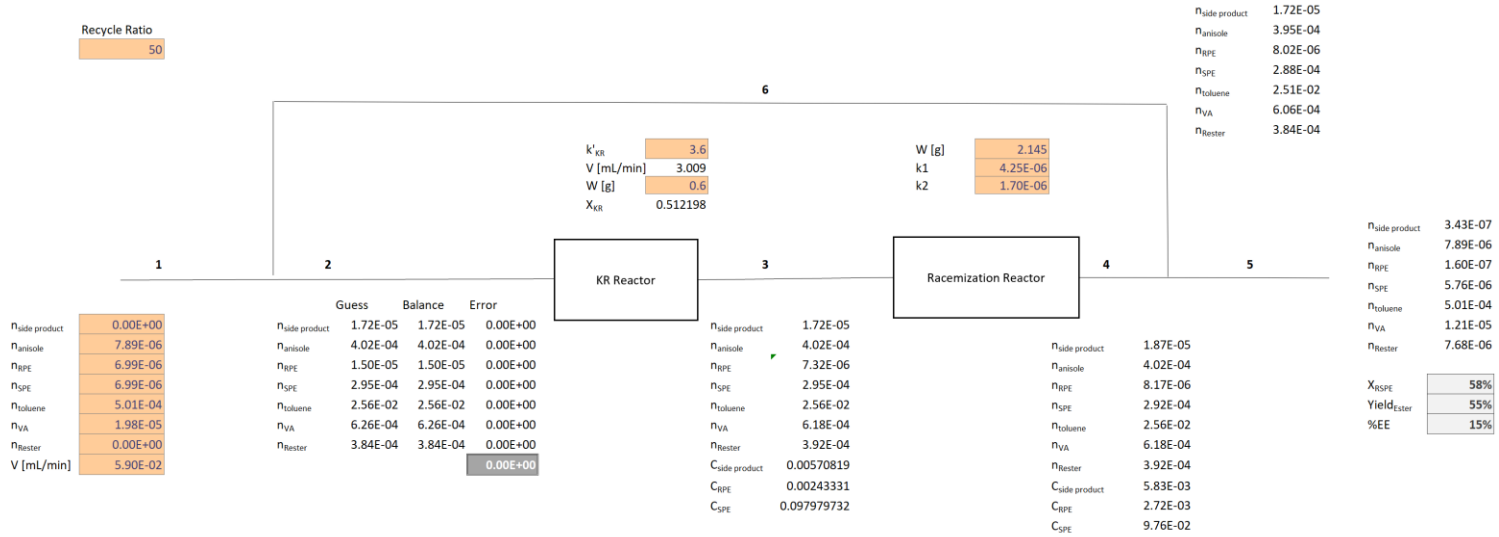

Balances around the KR reactor:

$$n_{RPE3} = n_{RPE2}(1 - X)$$

$$n_{Rester3} = n_{Rester2} + n_{RPE2}X$$

Balances around the RAC reactor:

$$C_{RPE4} = \left(e^{\frac{-[(W)(2k_1+k_2)}{\dot{V}}}\right)\left(\frac{C_{RPE3}}{2} - \frac{C_{SPE3}}{2}\right) + \frac{e^{\frac{-(k_2W)}{\dot{V}}}(C_{RPE3} + C_{SPE3})}{2}$$

$$C_{SPE4} = \frac{e^{\frac{-(k_2W)}{\dot{V}}}(C_{RPE3} + C_{SPE3})}{2} - \left(e^{\frac{-[W)(2k_1+k_2)}{\dot{V}}}\right)\left(\frac{C_{RPE3}}{2} - \frac{C_{SPE3}}{2}\right)$$

$$C_{side\ product\ 4} = C_{side\ product\ 3} + C_{RPE3} + C_{SPE3} - e^{\frac{-(k_2W)}{\dot{V}}}(C_{RPE3} + C_{SPE3})$$

Balances around recycle point for all species, I, with recycle ratio, R:

$$n_{i5} = \frac{n_{i4}}{1 + R}$$

$$n_{i6} = n_{i5}R$$

APPENDIX B – ReactIR Spectra

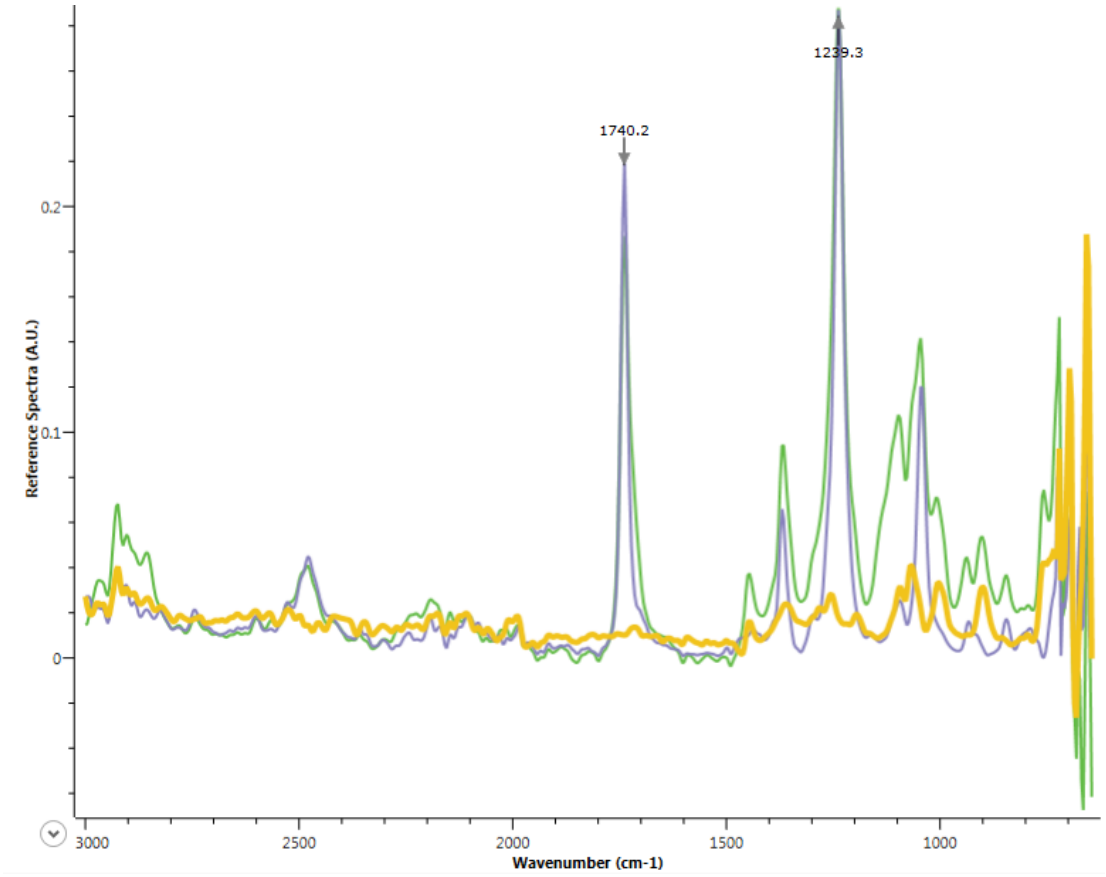

Figure 15: ReactIR spectra for ethyl acetate (green), vinyl acetate (purple), and R-1-phenylethylacetate (yellow).

APPENDIX C – GC Retention Times

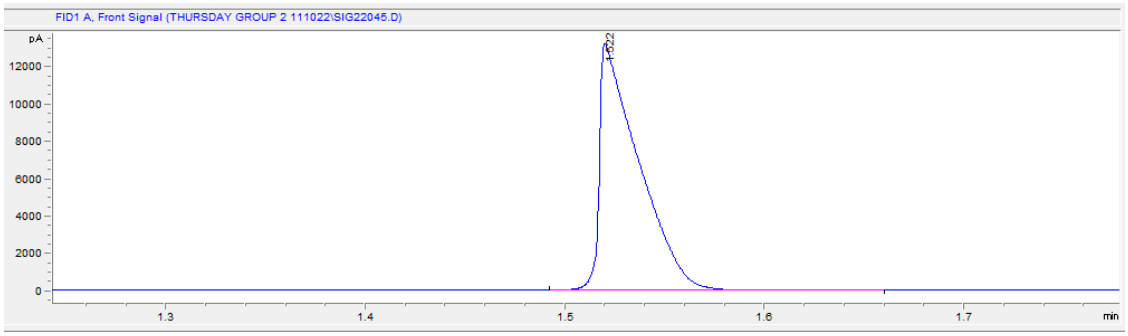

Figure 16: Toluene retention time

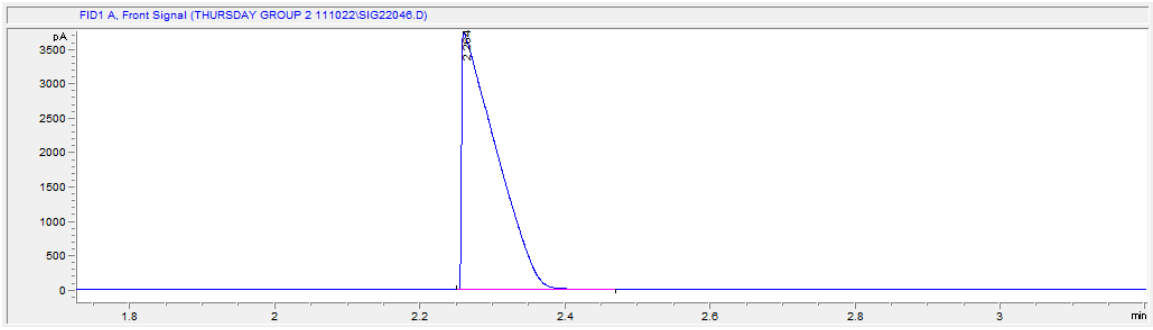

Figure 17: Anisole retention time

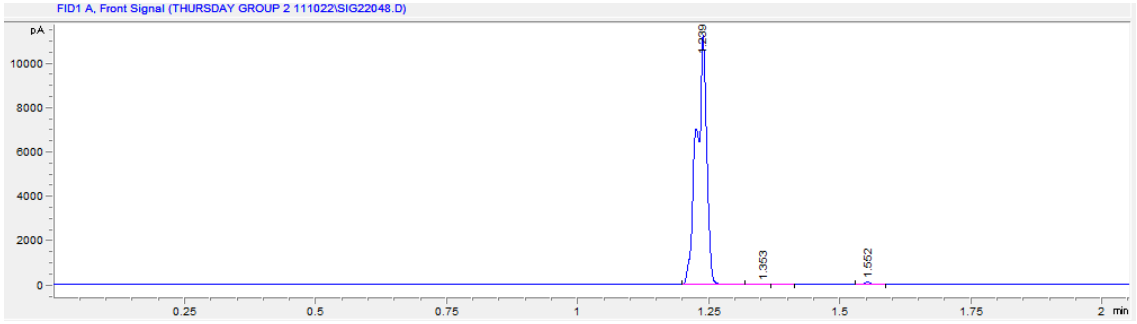

Figure 18: Ethyl Acetate retention time

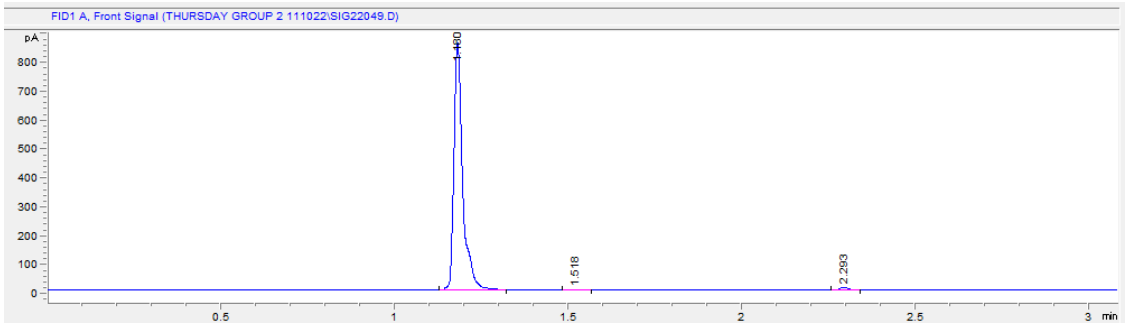

Figure 19: Vinyl Acetate retention time

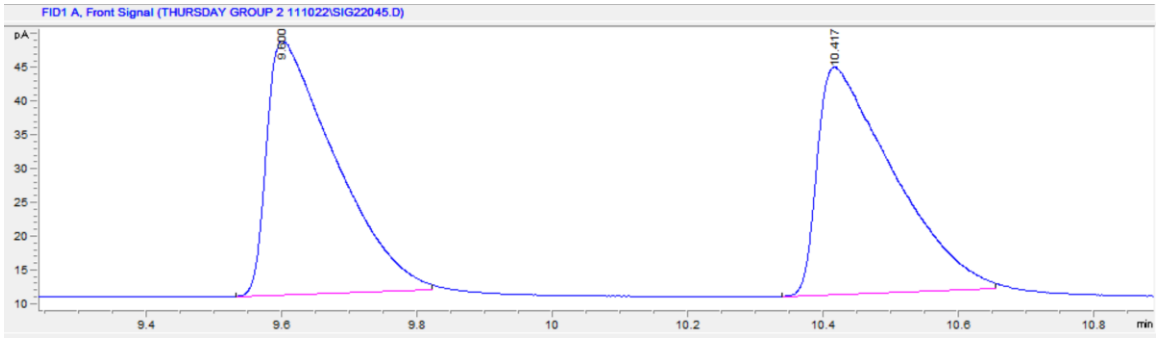

Figure 20: (R,S)-phenylethanol retention time

APPENDIX D – Calibration Curves

D1. IR Calibration Curves

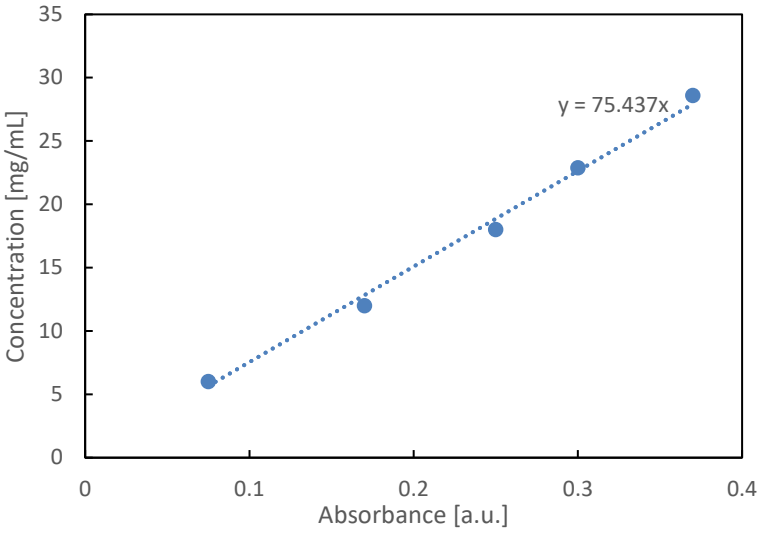

Figure 21: Vinyl acetate IR calibration curve

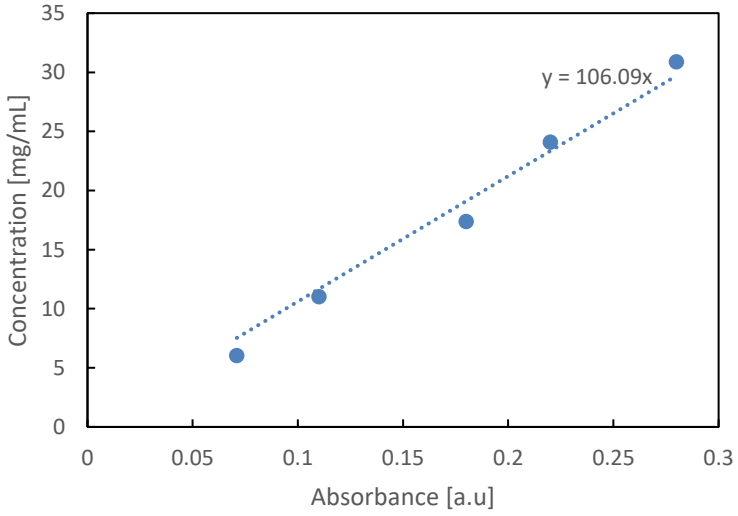

Figure 22: Ethyl acetate IR calibration curve

D2. GC-FID Calibration Curves

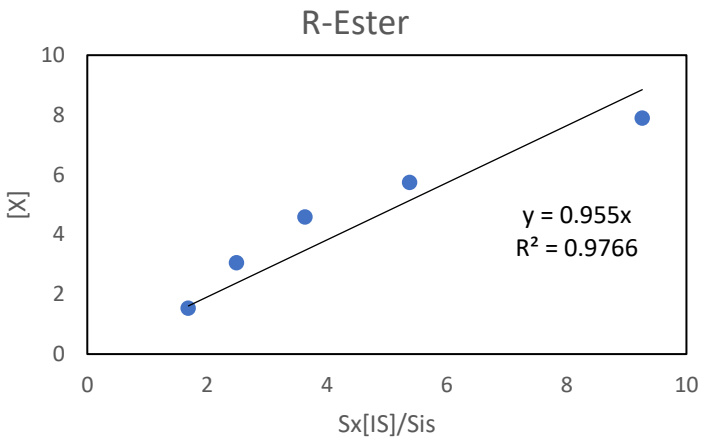

Figure 23: R-Ester GCFID calibration curve using anisole as internal standard.

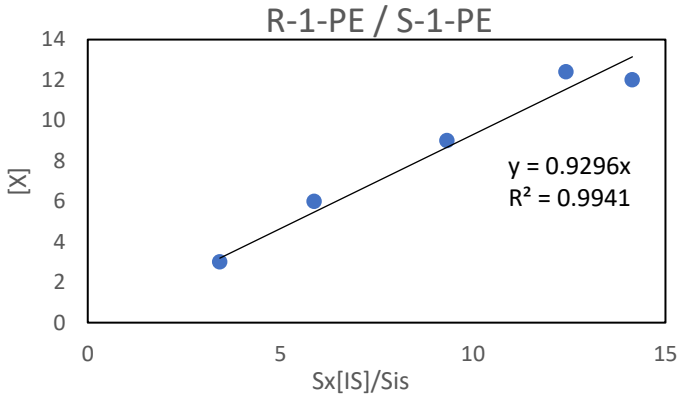

Figure 24: (R,S)-1-PE GC-FID calibration curve using anisole as internal standard.

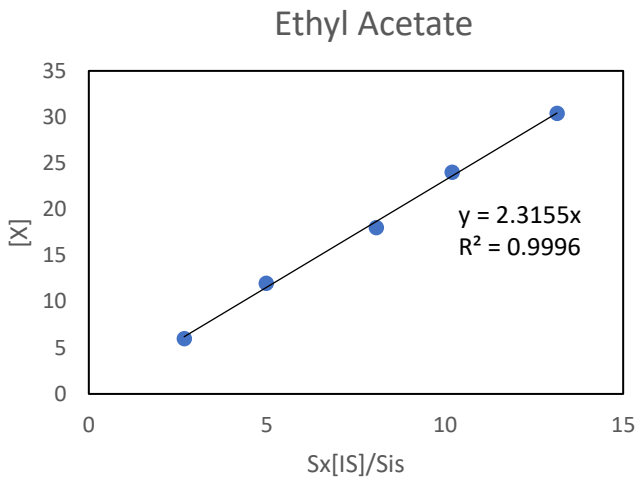

Figure 25: Ethyl Acetate GC-FID calibration curve using anisole as internal standard.

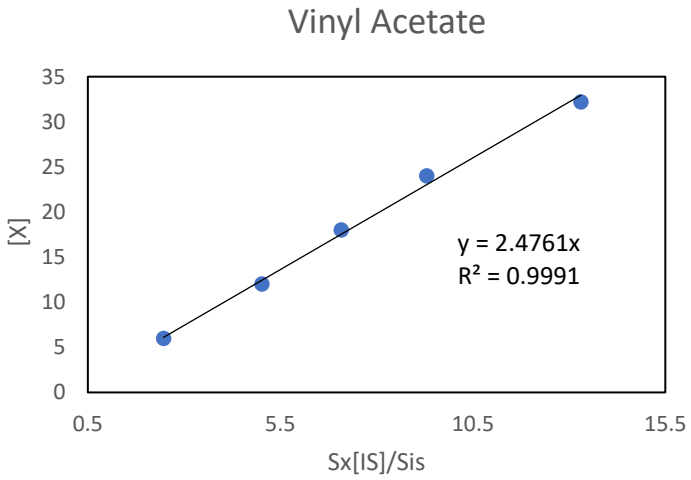

Figure 26: Vinyl acetate GC-FID calibration curve using anisole as internal standard.

APPENDIX E – Gas Chromatography Parameters

The following parameters were used for GCFID analysis:

Agilent 7820 GCFID instrument with 0.25 mm inner diameter and 25 m long Agilent CP-Chirasil-Dex CB GC column was used with split/splitless inlet, H_2 carrier gas at a 1:100 split ratio, injection volume of 0.6 μL, and an isothermal oven temperature of 110 °C, held for 20 minutes.

References

1. Annapurna Devi, N., Radhika, G., & Bhargavi, R. (2017). Lipase catalyzed transeterifcation of ethyl butyrate synthesis in n-hexane: a kinetic study. *J Food Sci Technol.*, 2871-2877.

2. Baumann, M., Moody, T. S., Smyth, M., & Wharry, S. (2020). A perspective on continuous flow chemistry in the pharmaceutical industry. *Org. Process Res. Dev.*, 1802-1813.

3. Bozan , A., SONGÜR, R., & MEHMETOĞLU, Ü. (2020, October 26). *The production of enantiomerically pure 1-phenylethanol by enzymatic kinetic resolution method using response surface methodology*. Retrieved from PMC PubMed Central: https://www.ncbi.nlm.nih.gov/pmc/articles/PMC7751928/

4. Catalano, S., Wozniak, A., & Kaplan, K. (2022). *Packed bed reactors*. Retrieved from Visual encyclopedia of chemical engineering equipment: https://encyclopedia.che.engin.umich.edu/packed-bed-reactors/

5. Cen, Y., Li, D., Xu, J., Wu, Q., Wu, Q., & Lin, X. (2018). Highly Focused Library-Based Engineering of Candida antarctica Lipase B with (S)-Selectivity Towards sec-Alcohols. *Advanced Synthesis & Catalysis*, 1-9. Retrieved from O.

6. Chen, B., Hu, J., Miller Elizabeth, E. M., Xie, W., Cai, M., & Gross, R. A. (2008, January 16). *Candida antarctica Lipase B Chemically Immobilized on Epoxy-Activated Micro- and Nanobeads: Catalysts for Polyester Synthesis* . Retrieved from ACS Publication: https://pubs.acs.org/doi/full/10.1021/bm700949x?openMendeleyModalAfterReload=true&selectedShareOption=#

7. Costa, L., Lamos, F., Reibeiro, F., & Cabral, J. (2008). Zeolite screening for racemization of 1-phenylethanol. *Catalysis Today*, 625-631.

8. de Miranda, A. S., de M. Silva, M. V., & Dias, F. C. (2017). Continuous flow dynamic kinetic resolution of rac-1-phenylethanol using a single packed-bed containing immobilized CAL-B lipase and VOSO4 as racemization catalysts. *React. Chem. Eng*, 375-381.

9. Fogler, S. H. (2020). *Elements of Chemical Reaction Engineering* (6 ed.). Pearson Technology Group.

10. Gihani, M. T., & Williams, J. M. (1999). Dynamic kinetic resolution. *Current Opinion in Chemical Biology*, 11-15.

11. Jensen, K. F. (2017). Flow chemistry—Microreaction technology comes of age. *AlChE Journal*, *63*(3), 858-869.

12. Kumar, A., Udugama, I. A., Gargalo, C. L., & Gernaey, K. V. (2020). Why is batch processing still dominating the biologics landscape? Towards an integreated continuous bioprocessing alternative. *Processes*, 1641.

13. Lee, S. L., O'Connor, T. F., & Yang, X. (2015). Modernizing pharmaceutical manufacturing: from batch to continuous production. *J Pharm Innov*, 191-199.

14. McCabe, W. L., Smith, J. C., & Harriott, P. (2005). *Unit Operations of Chemical Engineering.* New York, NY: McGraw Hill.

15. Mullaugh, K. (2020, October 20). *ChemLibretexts*. Retrieved from ChemLibretexts: https://chem.libretexts.org/Ancillary_Materials/Worksheets/Worksheets%3A_Analytical_Chemistry_II/Internal_Standards_and_LOD

16. Otvos, S. B., & Kappe, O. C. (2021). Continuous flow asymmetric synthesis of chiral active pharmaceutical ingredients and their advanced intermediates. *Green Chem*.

17. Roche, P., & Young, C. (2022). *Batch-to-continuous process intensification for small-molecule pharmaceutical manufacturing.* Worcester, MA: WPI.

18. Sigma Aldrich. (2022). *Lipase B Candida antartica immobilized on Immobead 150, recombinant from yeast*. Retrieved from Sigma Alrich: https://www.sigmaaldrich.com/US/en/product/sigma/52583?gclid=Cj0KCQiA4uCcBhDdARIsAH5jyUkVYV4gfz_X4F0Zkd2d3i3DewpMvrYcW4NuVQxRMjsGO6tUoykYbVsaAqduEALw_wcB&gclsrc=aw.ds

19. Stauch, B., Fisher, S. J., & Cianci, M. (2015, December). *Journal of Lipid Research* . Retrieved from Open and closed states of Candida antarctica lipase B: protonation and the mechanism of interfacial activation1: https://www.ncbi.nlm.nih.gov/pmc/articles/PMC4655990/#b3

20. Stephan Jaenicke, G. K.-L. (2007). Dynamic Kinetic Resolution Combining Enzyme and Zeolite Catalysis. *Elsevier*, Pages 313-316.

21. Wuyts, S., De Temmerman, K., De Vos, D., & Jacobs, P. (2005). Acid zeolites as alcohol racemization catalysts: Screening and application in biphasic dynamic kinetic resolution. *Chemistry Europe*, 386-397.

22. Zhu, Y. F.-L.-K. (2007). Dynamic Kinetic Resolution of Secondary Alcohols Combining Enzyme-Catalyzed Transesterification and Zeolite-Catalyzed Racemization. *https://doi.org/10.1002/chem.2006007*, Chem. Eur. J., 13: 541-547.

23. Zhu, Y., Fow, K.-L., Chuah, G.-K., & Jaenicke, S. (2006, December 19). *Dynamic Kinetic Resolution of Secondary Alcohols Combining Enzyme-Catalyzed Transesterification and Zeolite-Catalyzed Racemization.* Retrieved from Chemistry Europe: https://chemistry-europe.onlinelibrary.wiley.com/doi/full/10.1002/chem.200600723?saml_referrer